Malaysian Journal of Analytical Sciences (MJAS)
Published by Malaysian Analytical Sciences Society

MORPHOLOGICAL STUDIES OF SILICON CARBIDE THIN FILM DEPOSITED BY VERY HIGH FREQUENCY – PLASMA ENHANCED CHEMICAL VAPOUR DEPOSITION THROUGH GAS DILUTION ADJUSTMENT

(Kajian Morfologi Filem Nipis Silikon Karbida Yang Dimendapkan oleh Frekuensi Sangat Tinggi – Pemendapan Wap Kimia Dipertingkatkan Plasma dengan Melaraskan Pencairan Gas)

Zainur Atika Ibrahim, Muhammad Firdaus Omar*, Abd Khamim Ismail

Department of Physics, Faculty of Sciences,
Universiti Teknologi Malaysia, 81310 Skudai, Johor Bahru, Malaysia

**Corresponding author: firdausomar@utm.my*

Received: 15 December 2021; Accepted: 27 March 2022; Published: 30 October 2022

Abstract

Dilution of gas was deployed to investigate the surface morphology and the surface topography of Silicon Carbide (SiC) film deposited using Very High Frequency – Plasma Enhanced Chemical Vapour Deposition (VHF-PECVD) technique. The deposition process of SiC thin film was performed with 150 MHz excitation frequency and 20 W radio frequency (RF) power. The argon and hydrogen carrier gas dilution was set to 5 sccm. Silane (SiH_4) and methane (CH_4) functioned as precursor gases and their flow rates were fixed at 2 and 8 sccm, respectively. Direct observations revealed that the surface morphology of deposited nanostructured-silicon carbide (ns-SiC) films in all samples had layer-island structure with varied island density and size formation above the critical layer thickness. Next, surface topography and roughness of the deposited SiC films were examined using Atomic Force Microscopy (AFM) in non-contact mode. As a result, all samples displayed different roughness, surface topography structure, and average grain diameter.

Keywords: silicon carbide, plasma enhanced chemical vapour deposition, dilution gas

Abstrak

Pencairan gas digunakan untuk menyiasat morfologi permukaan dan topografi permukaan filem silikon karbida (SiC) yang dimendap menggunakan kaedah Frekuensi Sangat Tinggi – Pemendapan Wap Kimia Dipertingkatkan Plasma (VHF-PECVD). VHF-PECVD dikendalikan menggunakan frekuensi pengujaan 150 MHz pada kuasa gelombang radio (RF) 20 W. Sementara itu, pencairan gas pembawa argon dan hidrogen ditetapkan kepada 5 sccm. Gas pendahulu silane (SiH_4) dan metana (CH_4) masing-masing ditetapkan pada 2 dan 8 sccm. Pemerhatian langsung mendedahkan bahawa morfologi filem nanostruktur-silikon karbida (ns-SiC) yang dideposit dalam semua sampel mempamer sktruktur lapisan-pulau dengan ketumpatan pulau yang berbeza dan pembentukan saiz di atas ketebalan lapisan kritikal. Topografi permukaan dan kekasaran filem SiC yang dimendap diperiksa dengan Mikroskopi Daya Atom (AFM) dalam mod bukan sentuhan. Hasil kajian menunjukkan bahawa semua sampel mempunyai kekasaran struktur topografi permukaan dan diameter butiran purata yang berbeza.

.

Kata kunci: silikon karbida, pemendapan wap kimia dipertingkatkan plasma, gas pencairan

Introduction

Nanoscience and nanomaterial are the fastest growing research areas to date since the introduction to nanotechnology by Richard Feynman [1]. Material properties improve when the material is reduced to nanoscale [2-7]. The cutting-edge trend of nanomaterial applications includes electronic devices for extreme environments such as high temperature, high corrosion, high nuclear radiation, and high electromagnetic radiation - the importance of using unique material as resource in extreme conditions. Silicon carbide (SiC) is a relatively new semiconductor material that has been gaining popularity in high-frequency and high-power applications. Since several decades ago, SiC has been identified as a potential material for use in extreme conditions due to its mechanical properties, chemical inertness, thermal stability, high oxidation resistance, high hardness, large band gap, and relatively lightweight [1, 8-11]. In fact, SiC has a crucial role in some optoelectronic device applications [11-13], including light-emitting diodes (LEDs), electroluminescent devices [14], and thermoelectric cooling (TEC) devices [15]. Nevertheless, low-quality material has hindered the development of high-quality devices [16].

Several methods that can be used to synthesise SiC thin films are hot wall chemical vapour deposition (HWCVD), plasma enhanced CVD (PECVD), electron cyclotron resonance CVD (ECR-CVD), magnetron sputtering, pulsed laser deposition (PLD), ion implantation, and molecular beam epitaxy (MBE) [8, 17]. Many studies revealed that high-quality thin films and nanostructured-SiC (ns-SiC) can be produced using higher radio frequency (RF) PECVD at lower temperature. Notably, PECVD with RF exceeding 13.56 MHz is classified as very high frequency (VHF-PECVD) [19].

The VHF-PECVD technique was employed in this study at 150 MHz plasma excitation frequency to deposit SiC film. The effect of dilution gas on SiC film was examined and characterised by using FTIR spectroscopy, FESEM, and AFM. Notably, high excitation frequency of PECVD has some advantages over conventional PECVD, including higher deposition rate, less defect and better-quality films, higher electron density, lower plasma potential, and lower impact of ion bombardment when compared to conventional PECVD [19]. However, no study has assessed SiC film synthesised with RF-PECVD at a frequency exceeding 100 MHz with SiH_4 and CH_4 precursors at low temperature. The ns-SiC thin film should successfully grow using VHF-PECVD at the said excitation frequency.

Materials and Methods

First, Si [100] substrates were thoroughly cleaned with ethanol and followed by organic cleaning in ultrasonic bath for 10 minutes. Next, the substrates were immersed in acetone for 10 minutes in ultrasonic bath. To remove the remaining contaminant particles, the substrates were submerged in 50% sulphuric acid (H_2SO_4) before another ultrasonic bath for 10 minutes. The oxide layer on the substrate surface was stripped off by immersing in 50% fluoric acid (HF). Finally, the substrates were rinsed with deionised (DI) water and blow-dried with N_2 gas. The substrates were then ready to be placed in the process chamber.

The substrates were labelled as samples A, B, and C. Sample A was diluted with the mixture of argon and hydrogen gases, while sample B was diluted only with hydrogen gas, and sample C without dilution of gas mixture. Substrate temperature, RF power, deposition time, and SiH_4 flow rate were fixed at 400 °C, 20 W, 15 minutes, and 2 sccm, respectively, for all samples A-C. The growth parameters for samples A-C are summarised in Table 1.

Table 1. Gas dilution growth parameter

Sample	Power (W)	Temperature (°C)	Argon Flow Rate (sccm)	Hydrogen (sccm)	Silane Flow Rate (sccm)	Methane Flow Rate (sccm)	Deposition Time (min)
A			5	5			
B	20	400	-	5	2	8	15
C			-	-			

Results and Discussion

Both chemical composition and bonding structure of Si C thin film samples were verified using IR spectroscop y. This technique has been vastly used to qualitatively a ssess the type of chemical bonding present in thin film materials, including a-Si:H, a-SiO_2, a-SiNx:H, a-SiCx: H, and a-C:H. In fact, IR spectroscopy is used to quanti tatively determine the concentration of terminal hydrog en bonds (Si-H, C-H, O-H, & N-H) and network bonds (Si-C, Si-O, Si-N, P-O, & B-O) present in thin film mat erials.

Figure 1 illustrates the IR spectrum for samples A-C in two regions ranging from 650 to 1500 cm^{-1} and 1800 to 3000 cm^{-1}. The sharp peaks observed at 1500-1800 cm^{-1} range are attributed to O-H water vapour vibration in t he air during the measurement [20, 25]. Moreover, sign als of the deposited thin film were noted at 650-1500 c m^{-1} and 1800-3000 cm^{-1}, in comparison to the blank Si wafer.

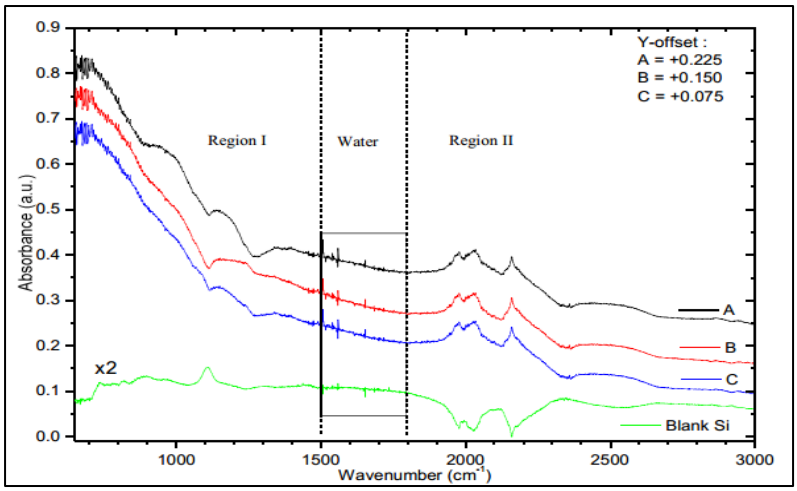

Figure 1. Comparison of IR spectrum between Si wafer and samples A-C

Spectra in regions (I) and (II) revealed the following vibrational bands: absorption band at ~ 650-1000 cm^{-1} is correlated to Si-C stretching [18, 21, 26-28]. The band at ~ 1000-1150 cm^{-1} is ascribed to Si-O-Si asymmetry and symmetry stretching vibration band or Si-CH_2-Si wagging mode [18, 21, 26, 28]. At ~ 1000 cm^{-1}, the band corresponds to Si-CH_n bending mode [24, 27]. In most samples, lower intensity absorption bands in the range of 1200-1500 cm^{-1} were detected. A shoulder at ~ 1250 cm^{-1} is linked with Si-CH_3 stretching mode [26] or Si-CH_n wagging mode [24]. The symmetry and asymmetry C-H_n bending and stretching modes are associated with ~ 1250-1500 cm^{-1} and 2700-3000 cm^{-1} bands, respectively [20-22, 26-27]. The Si-H_n stretching mode is assigned to the band from ~ 1850 cm^{-1} to 2300 cm^{-1} [21]. The small sharp peak at ~ 2350 cm^{-1} is attributed to CO_2 in the atmosphere [24, 27]. All the peaks verified that all the deposited thin film samples possessed Si-C

network bonds.

Scanning electron microscopy

Figures 2 (a-c) illustrate the overall surface morphology of the thin films, with inset images zooming in on the flat region for samples A-C respectively. Next, Figures 2 (i-iii) portray the cross-sectional morphology for samples A-C respectively. In sample A, the thin film had the largest island diameter at less than 1 µm and the film thickness was roughly ~ 397 nm. The island diameter in sample B was similar to that of sample A. However, the size exceeded 1 µm when agglomeration occurred among the islands. Sample B had thinner film thickness than sample A at 337 nm. Without argon gas during deposition, the density of island nucleation displayed an increase in sample B, when compared to sample A. Meanwhile, sample C showed the highest density of island nucleation above the film surface after attaining critical thickness. Notably, island formation increased in sample B and island density was higher in sample C. Therefore, dilution gas was proven effective to reduce the C-H network, which is ascribed to the high dissociation of methane on the films [23]. The film thickness values obtained from FESEM were 397 nm, 337 nm, and 357 nm for samples A-C respectively.

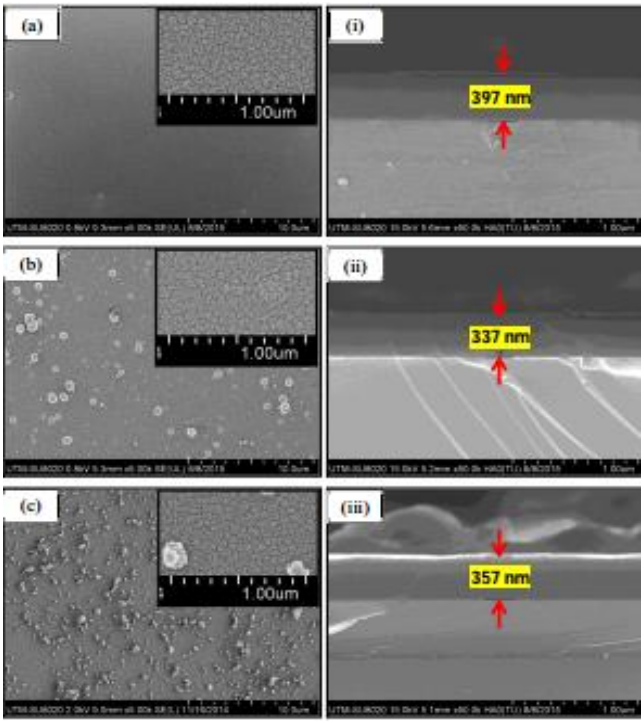

Figure 2. FESEM images of surface morphology ((a), (b), & (c)) and cross-sectional view ((i), (ii), & (iii)) of SiC films grown with different types of gas carriers for samples A, B, and C, respectively

Atomic force microscopy

Figure 3 shows high resolution surface topography of AFM images for samples A-C represented in root-mean-square roughness (R_{rms}). Sample B had smoother surface with R_{rms} of 0.798 nm, when compared to samples A and C with R_{rms} values of 1.505 nm and 1.599 nm, respectively. Dilution gas influenced the formation of different grain structure shapes, including triangular base pyramid [29, 31], square plateaus [30, 32], and semi-square plateaus for samples A-C respectively. This result is ascribed to the phase transition from amorphous to crystalline phase when hydrogen and argon were added during the deposition process [23]. Upon comparing the R_{rms} values of samples A and B, higher surface roughness in sample A is attributed to the effect of argon ion bombardment on film surface, although the

deposition pressure in sample A was lower than that of sample B. Hydrogen ions that existed in sample B deposition process could have less ion bombardment effect due to high electronegativity of H ion to have reaction in gas space with other reactants, when compared to the behaviour of argon ions as inert gas naturally. The mean diameter value of triangular pyramid island was ~ 81 nm and sample B showed well definite square plateaus of ~ 120 nm wide (based). For sample C, it had no perfect square plateau shape of each grain and the average wide of grain was ~ 140 nm.

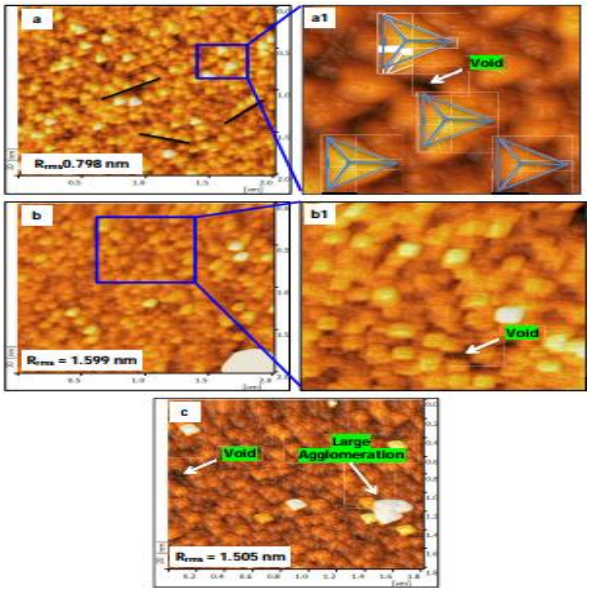

Figure 3. AFM images of the surface topography of SiC films grown with different types of gas carriers for samples A, B, and C represented by (a & a1), (b & b1), and (c), respectively

Conclusion

In conclusion, the surface morphology of the deposited ns-SiC films revealed a layer-island structure with varied island density and size formation above the critical layer thickness in all samples. Both surface topography and roughness of the deposited SiC films were assessed using non-contact AFM mode. The results revealed that all samples had different roughness, surface topography structure, and average grain diameter. Thin film deposited with dilution gas had a very smooth surface with the lowest R_{rms} value of 0.798 nm. Notably, dilution gas had affected the formation of different grain structure shapes. Nonetheless, the role of argon gas in changing the grain structure from square plateaus to triangular base pyramid demands further investigation.

Acknowledgement

The authors gratefully acknowledge the financial supported by Universiti Teknologi Malaysia, under Collaborative Research Grant National (CRG) (Vot no: R.J130000.7354.4B523) and UTM-TDR, Registration Proposal No: PY/2018/03249 (Vot no: Q.J130000. 3554.06G21). We are thankful to Physics Department, Faculty of Sciences, Universiti Teknologi Malaysia and Ibnu Sina Institute for providing the experimental facilities.

References

1. Bandyopadhyay, A. K. (2008). Nano Materials. New Age International (P) Ltd, New Delhi.
2. Tritt, T. M. and Subramanian, M. A. (2006). Thermoelectric materials, phenomena, and applications: a bird's eye view. *MRS Bulletin*, 31(3): 188-198.

3. J. J. and Wang, J. N. (2007). An approach to the synthesis of silicon carbide nanowires by simple thermal evaporation of ferrocene onto silicon wafers. *European Journal of Inorganic Chemistry*, 2007 (25): 4006-4010.
4. Huczko, A., Bystrzejewski, M., Lange, H., Fabianowska, A., Cudziło, S., Panas, A. and Szala, M. (2005). Combustion synthesis as a novel method for production of 1-D SiC nanostructures. *The Journal of Physical Chemistry B*, 109(34): 16244-16251.
5. Huczko, A., Lange, H., Bystrzejewski, M., Rűmmeli, M. H., Gemming, T., & Cudziło, S. (2005). Studies on spontaneous formation of 1D nanocrystals of silicon carbide. *Crystal Research and Technology: Journal of Experimental and Industrial Crystallography*, 40(4-5): 334-339.
6. Hamashita, D., Miyajima, S. and Konagai, M. (2012). Preparation of Al-doped hydrogenated nanocrystalline cubic silicon carbide by VHF-PECVD for heterojunction emitter of n-type crystalline silicon solar cells. *Solar Energy Materials and Solar Cells*, 107: 46-50.
7. Zhou, W., Zhang, Y., Niu, X., & Min, G. (2008). One-dimensional SiC nanostructures: Synthesis and properties. In *One-Dimensional Nanostructures* (pp. 17-59). Springer, New York, NY.
8. Kamble, M. M., Waman, V. S., Mayabadi, A. H., Ghosh, S. S., Gabhale, B. B., Rondiya, S. R., ... and Jadkar, S. R. (2014). Hydrogenated silicon carbide thin films prepared with high deposition rate by hot wire chemical vapor deposition method. *Journal of Coatings*, 2014: 1-11.
9. Pearton, S. J. and Ren, F. (2013). Wide bandgap semiconductor one-dimensional nanostructures for applications in nanoelectronics and nanosensors. *Nanomaterials and Nanotechnology*, 3: 1-15.
10. Neudeck, P. G. (2007). SiC technology. in The VLSI Handbook, 2nd ed. CRC Press, Boca Raton, Florida: pp. 5.1-5.34.
11. Harris G. L. (1995). Properties of silicon carbide. INSPEC, The Institution of Electrical Engineers, London, United Kingdom: pp. 3-9.
12. Palmour, J. W., Edmond, J. A., Kong, H. S. and Carter Jr, C. H. (1993). 6H-silicon carbide devices and applications. *Physica B: Condensed Matter*, 185(1-4): 461-465.
13. Sheng, S., Spencer, M. G., Tang, X., Zhou, P., Wongchotigul, K., Taylor, C. and Harris, G. L. (1997). An investigation of 3C-SiC photoconductive power switching devices. *Materials Science and Engineering: B*, 46(1-3): 147-151.
14. Saddow S. and Agarwal A. (2004). Advances in silicon carbide processing and applications. Artech House, Inc., Boston, London.
15. Zorman, C. A. and Parro, R. J. (2008). Micro-and nanomechanical structures for silicon carbide MEMS and NEMS. *Physica Status Solidi (b)*, 245(7): 1404-1424.
16. Willander, M., Friesel, M., Wahab, Q. U. and Straumal, B. (2006). Silicon carbide and diamond for high temperature device applications. *Journal of Materials Science: Materials in Electronics*, 17(1): 1-25.
17. Avram, M., Avram, A., Bragaru, A., Chen, B., Poenar, D. P., & Iliescu, C. (2010, October). Low stress PECVD amorphous silicon carbide for MEMS applications. In *CAS 2010 Proceedings (International Semiconductor Conference,* 1: pp. 239-242.
18. Künle, M., Hartel, A., Löper, P., Janz, S. and Eibl, O. Nanostructure and phase formation in annealed a-Si1-xCx: H thin films for advanced silicon solar cells. *21st Workshop on Quantum Solar Energy Conversion (QUANTSOL)*: pp. 1-4.
19. Hamidinezhad, H., Wahab, Y. and Othaman, Z. (2011). Ultra-sharp pointed tip Si nanowires produced by very high frequency plasma enhanced chemical vapor deposition via VLS mechanism. *Journal of Materials Science*, 46(15), 5085-5089.
20. Socrates G. (2004). Infrared and raman characteristic group frequencies: Tables and charts. 3rd edition. John Wiley & Son Ltd.
21. King, S. W., French, M., Bielefeld, J. and Lanford, W. A. (2011). Fourier transform infrared spectroscopy investigation of chemical bonding in low-k a-SiC: H thin films. *Journal of Non-*

Crystalline Solids, *357*(15), 2970-2983.

22. Gates, S. M., Neumayer, D. A., Sherwood, M. H., Grill, A., Wang, X. and Sankarapandian, M. (2007). Preparation and structure of porous dielectrics by plasma enhanced chemical vapor deposition. *Journal of Applied Physics*, 101(9): 094103-1-094103-8.
23. Gradmann, R., Loeper, P., Künle, M., Rothfelder, M., Janz, S., Hermle, M and Glunz, S. (2011). Si and SiC nanocrystals in an amorphous SiC matrix: Formation and electrical properties. *Physica Status Solidi C*, 8(3): 831-834.
24. Kim, Y. T., Yoon, S. G., Kim, H., Suh, S. J., Jang, G. E., & Yoon, D. H. (2005). Crystallization of a-Si: h and a-SiC: h thin films deposited by PECVD. *Journal of Ceramic Processing & Research*, 6(4): 294-297.
25. Chen, E., Du, G., Zhang, Y., Qin, X., Lai, H. and Shi, W. (2014). RF-PECVD deposition and optical properties of hydrogenated amorphous silicon carbide thin films. *Ceramics International*, 40(7): 9791-9797.
26. Kuznetsov V. L. and Butenko Y. V. (2006). Diamond phase transitions at nanoscale in ultrananocrystalline diamond: Synthesis, properties and applications. William Andrew Publishing, New York: pp. 405-475.
27. Lin, Z., Guo, Y., Song, C., Song, J., Wang, X., Zhang, Y., ... and Huang, X. (2015). Influence of the oxygen content in obtaining tunable and strong photoluminescence from low-temperature grown silicon oxycarbide films. *Journal of Alloys and Compounds*, 633: 153-156.
28. Peri, B., Borah, B. and Dash, R. K. (2015). Effect of RF power and gas flow ratio on the growth and morphology of the PECVD SiC thin film s for MEMS applications. *Bulletin of Materials Science*, 38(4): 1105-1112.
29. El Khalfi, A. I., Ech-chamikh, E. M., Ijdiyaou, Y., Azizan, M., Essafti, A., Nkhaili, L. and Outzourhit, A. (2014). Infrared and Raman study of amorphous silicon carbide thin films deposited by radiofrequency cosputtering. *Spectroscopy Letters*, 47(5): 392-396.
30. ElGazzar, H., Abdel-Rahman, E., Salem, H. G. and Nassar, F. (2010). Preparation and characterizations of amorphous nanostructured SiC thin films by low energy pulsed laser deposition. *Applied Surface Science*, 256(7): 2056-2060.
31. Bosi, M., Attolini, G., Negri, M., Frigeri, C., Buffagni, E., Ferrari, C., ... and Verucchi, R. (2013). Optimization of a buffer layer for cubic silicon carbide growth on silicon substrates. *Journal of Crystal Growth*, 383: 84-94.
32. Radmilovic, V., Dahmen, U., Gao, D., Stoldt, C. R., Carraro, C. and Maboudian, R. (2007). Formation of< 111> fiber texture in β-SiC films deposited on Si (100) substrates. *Diamond and Related Materials*, 16(1): 74-80.
33. Wu, X. L., Gu, Y., Xiong, S. J., Zhu, J. M., Huang, G. S., Bao, X. M. and Siu, G. G. (2003). Self-organized growth and optical emission of silicon-based nanoscale β-SiC quantum dots. *Journal of Applied Physics*, 94(8): 5247-5251.